Thang, M., Dondon, L., Thang, D., & Rether, B. (1972) *FEBS Lett. 26*, 145–150.
Wagner, T., & Sprinzl, M. (1980) *Eur. J. Biochem. 108*, 213–221.
Weissbach, H., Redfield, B., & Brot, N. (1978) *Arch. Biochem. Biophys. 145*, 676–684.
Wittinghoffer, A., Frank, R., & Leberman, R. (1980) *Eur. J. Biochem. 108*, 423–431.

Irreversible Binding of Phage φX174 to Cell-Bound Lipopolysaccharide Receptors and Release of Virus–Receptor Complexes†

Nino Leonard Incardona*
Department of Microbiology and Immunology, University of Tennessee Center for Health Sciences, Memphis, Tennessee 38163
Jean Kuehl Tuech
Biology Department, Christian Brothers College, Memphis, Tennessee 38104
Gopal Murti
Division of Virology and Molecular Biology, St. Jude Children's Research Hospital, Memphis, Tennessee 38101
Received February 5, 1985

ABSTRACT: At 37 °C, binding of φX174 to the lipopolysaccharide receptors in the outer membrane of *Escherichia coli* C is followed by an irreversible ejection of its DNA. DNA ejection marks the beginning of the eclipse period in the infection cycle. Binding data with a φX mutant F*cs*70 at 15 °C, where the DNA ejection, or eclipse, rate is essentially zero, do not follow the law of mass action. This rules out a simple mechanism of reversible binding followed by irreversible DNA ejection. A more complex reaction model was devised to fit the data [Incardona, N. L. (1983) *J. Theor. Biol. 105*, 631–645]. It takes into account the fact that lipopolysaccharide-containing outer membrane fragments are continually released from infected *E. coli* cells, some of which have φX bound to them. In this paper the model is shown to fit the binding data for wild-type virus at 15 °C and to account for the nonlinearity observed at 37 °C in the pseudo-first-order binding kinetics and first-order eclipse kinetics for both mutant and wild-type virus. This leads to the conclusion that φX174 binding to cell-bound receptors is irreversible but binding to released receptors is reversible. The release of virus–receptor complexes from infected cells and the dissociation of these complexes were confirmed by electron microscopy. We propose that initially a single φX174 vertex interacts reversibly with *E. coli* lipopolysaccharide but dissociation from the cell is prevented by the subsequent interaction of additional vertices with adjacent receptor molecules.

Protein–protein and protein–nucleic acid interactions play a central role in stabilizing the nucleocapsid structure of most viruses, particularly in their extracellular form. In the case of φX174, the isometric single-stranded DNA phage, a specific set of noncovalent interactions must be rapidly broken when the phage binds to its LPS[1] receptor in the bacterial outer membrane and ejects its DNA into the periplasmic space. Since binding and DNA ejection occur with purified LPS (Incardona & Selvidge, 1973), these virus–receptor interactions can be used to characterize mutationally induced alterations in tertiary and quaternary structure of the viral capsid proteins that are involved in the delivery of the viral genome into the cell.

The icosahedral capsid φX has a single capsomere at each of the 12 vertices. If all capsomeres are identical, each would be composed of a single H protein surrounded by five molecules each of F and G proteins with the G and H proteins on the external surface of the capsid (Burgess, 1969; Edgell et al., 1969; Siden & Hayashi, 1974). The 60 J proteins are required for DNA packaging into preformed proheads, suggesting an internal location (Aoyama et al., 1981). Several, if not all, molecules of the gene H protein are injected along with the viral DNA (Jazwinski et al., 1975b), and *cs*70, a mutation located in gene F (Hutchison et al., 1972), leads to a defect in DNA injection (Incardona, 1974; Segal & Dowell, 1974). Thus, at least two of the four structural proteins are involved in DNA penetration of the outer-membrane.

Newbold & Sinsheimer (1970a,b) developed a technique for measuring the kinetics of the partial DNA ejection or eclipse reaction for φX bound to intact cells. We analyzed the temperature dependence of the reaction rate in terms of Arrhenius kinetic theory for wild-type phage and two types of mutants, those having amino acid substitutions in the capsid proteins and those having deleted or inserted sequences in the DNA (Incardona & Müller, 1985). However, it became clear that the reversibility of the binding step could be altered by these mutations. Therefore, a study of the binding of φX174

† Supported by National Science Foundation Grant PCM77-15982, the Robert Rizzo Memorial Research Fund (N.L.I.), Cancer Center Support Grant CA21765, and American Lebanese Syrian Associated Charities (G.M.).

[1] Abbreviations: LPS, lipopolysaccharide; EDTA, ethylenediaminetetraacetic acid; cs, cold sensitive; am, amber; SVB, starvation buffer; PFU, plaque-forming unit; Tris, tris(hydroxymethyl)aminomethane.

0006-2960/85/0424-6439$01.50/0

to *Escherichia coli* cells was undertaken to ascertain whether any steps preceeding the irreversible eclipse reaction are reversible.

An earlier study by Fujimura & Kaesberg (1962) addressed this question, but most of their binding studies were done at temperatures where the rate of the irreversible eclipse reaction precludes drawing any conclusion concerning the preceding steps. Since the F*cs*70 mutation results in an eclipse rate close to zero at 15 °C (Incardona, 1974), the reversibility of ϕX binding to cells was examined with the mutant at that temperature (Incardona, 1983b). The data rule out a simple mechanism of reversible binding of ϕX to a single class of receptors followed by an irreversible eclipse reaction, but we were able to fit the data to the following two-step, two interconnecting pathway model:

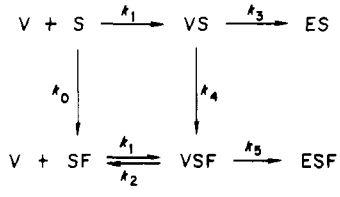

(1)

where S represents cell-bound receptor sites and SF are released or free sites.

The novel feature of this reaction mechanism is that it takes into account the dynamic state of the bacterial outer membrane (Muhlradt & Menzel, 1974; Osborn et al., 1980). It provides for the release of LPS receptors from cells as either unoccupied sites, SF, or with bound virus, VSF. It also incorporates the fact that ϕX can bind to and eclipse on purified LPS receptors, the V + SF to ESF pathway (Incardona & Selvidge, 1973; Jazwinski et al., 1975a). In this paper we show that this same model can account for the nonlinear pseudo-first-order binding kinetics and the biphasic first-order eclipse kinetics observed at 37 °C. Moreover, the model predicts that the experimentally observed differences between wild-type ϕX and the F*cs*70 mutant are due to the mutant's lower rate constants for three of the seven reactions in eq 1: the eclipse reaction on both cell-bound and free receptors and the dissociation of virus from free receptors. However, irreversible binding to cell-bound receptors is not altered by the F*cs*70 mutation.

Materials and Methods

Viral and Bacterial Strains. Wild-type ϕX174 and the lysis-defective amber mutant E*am*3 were originally obtained from R. Sinsheimer while C. Dowell provided the eclipse mutants F*cs*70 and E*am*3F*cs*70. The *cs*70 mutation is in the 75% C-terminal portion of gene F (Sanger et al., 1978). *Escherichia coli* C and a spontaneous phage T1 resistant mutant, C/1, were the amber nonsuppressor strains used, and HF4714 was the *sup*$^+$ strain. As a control for nonspecific binding, C/ϕX was routinely employed. A summary of most phage and host strain phenotypes can be found in Benbow et al. (1971). A few binding experiments were performed with insertion and deletion mutants of E*am*3, J-F *ins*11, and J-F *del*3, constructed by Müller & Wells (1980).

Media and Buffers. KC broth has 10 g of tryptone and 5 g of KCl/L of water, and KC+Ca broth has, in addition, 1 mL of 1.0 M $CaCl_2$ added prior to sterilization. In the case of TYE, each liter contains 10 g of tryptone, 5 g of yeast extract, 5 g of NaCl, and 3 g of KCl. The top and bottom agars for plaque assays were prepared by adding 15 and 11 g of agar to TYE, respectively (Müller & Wells, 1980). The composition of Cas is 15 g of casamino acids, 3 g of glycerol, 10.5 g of $Na_2HPO_4 \cdot 7H_2O$, 4.5 g of KH_2PO_4, 1.0 g of NH_4Cl, 0.3 g of $MgSO_4$, and 1 mL of 1% gelatin per liter. SVB starvation buffer, EDTA–borate elution buffer, and PO_4 dilution buffer have been previously described (Incardona & Selvidge, 1973; Rueckert & Zillig, 1962). Borate buffer is a saturated solution of sodium tetraborate at 2 °C.

Growth, Purification, and Plaque Assay of ϕX174. High-titer crude lysates were prepared by growing either C/1 or HF4714 in TYE and by infecting with a fresh plaque after adding sterile $CaCl_2$ to a final concentration of 1 mM as previously described (Incardona, 1981a). Titers above 1×10^{10} PFU/mL were routinely obtained, and the reversion frequency of each marker was between 10^{-4} and 10^{-6}.

When purifying ϕX strains containing the E*am*3 mutation, we grew C or C/1 in Cas at 37 °C to 1×10^8 cells/mL, infected with a multiplicity of 5–10 after addition of $CaCl_2$ to a 1.0 mM concentration, and harvested the infected cells by centrifugation at 2–3-h postinfection. The pellet from a 50-mL culture was resuspended in 2.10 mL of borate buffer and lysed at room temperature by the addition of 600 μL of 0.15 M EDTA, pH 7, and 300 μL of Sigma egg white lysozyme. After 15 min the suspension was frozen and thawed 3 times in a dry ice–acetone bath, sonicated for 1 min to reduce the viscosity, and centrifuged at 27000*g* for 15 min. The supernatant solution was then layered on a 5–25% (w/w) sucrose gradient made with a 1.0 M NaCl and 0.0125 M EDTA–borate buffer, pH 9.1. Centrifugation was at 5 °C for 40 min at 50000 rpm in the VTi50 vertical tube rotor of the Beckman L5-50 ultracentrifuge. After fractions were collected from a hole punctured in the bottom of the centrifuge tube, the virus-containing fractions were located by absorbance readings at 260 nm of diluted aliquots. The remainder of the undiluted virus-containing fractions was pooled and stored at 5 °C. If further purification was desired, the sucrose fractions were diluted about 1:10 with borate buffer, and sufficient dry, optical-grade CsCl was added to give a final density of 1.36 g/mL. The sample was centrifuged to equilibrium at 5 °C in the VTi50 rotor at 50000 rpm. The virus-containing fractions were immediately dialyzed against borate buffer to remove the CsCl. The PFU/particle ratio of virus-containing fractions from both the sucrose and CsCl gradients was 0.25. A comparison was made of cultures infected at two cell densities, 1×10^8 and 4×10^8 cells/mL. The final yield per infected cell at the sucrose gradient step was 2-fold higher at the lower cell density, a difference that persisted from 1- to 3.5-h postinfection.

Cells for the plaque assay were grown in TYE to almost 1×10^9 cells/mL. The virus samples were diluted with PO_4 dilution buffer at room temperature and plated out with 0.2 mL of cells within 10 min after dilution. Sterile $CaCl_2$ was added to the melted top agar to give a final concentration of 5 mM. The conditions for counting the plaques with an automatic colony counter have already been described (Incardona, 1981a).

Binding Kinetics. E. coli C/1 and C/ϕX cells were grown in KC+Ca to 2×10^8 cells/mL, washed once with an equal volume of cold SVB, resuspended in $^1/_{10}$ volume of SVB, and maintained on ice. The ϕX samples were diluted with borate buffer to 1×10^{10} PFU/mL. In the case of sucrose gradient fractions, an overnight dialysis against the same buffer was included. Prior to mixing of the virus and cells, the virus was diluted 10-fold in SVB and incubated at 37 °C for 30 min (Incardona, 1981a) while the cells were diluted to the desired cell density and preincubated at the desired temperature for 15 min. The binding reaction was usually initiated by a 1:100 dilution of the preincubated virus, and aliquots were rapidly

Table I: Rate Constants for the Reaction Model in Equation 1

	values used in model (min^{-1})			
	15 °C		37 °C	
constant	wild type	Fcs70	wild type	Fcs70
k_0	1.0×10^{-3}	1.0×10^{-3}	$1.5\ (5.0 \times 10^{-2})$	$1.5\ (5.0 \times 10^{-2})$
k_4	1.0×10^{-3}	1.0×10^{-4}	$1.5\ (5.0 \times 10^{-2})$	$1.5\ (5.0 \times 10^{-2})$
k_1	3.0×10^{-13} [a]	3.0×10^{-13} [a]	1.5×10^{-12} [a]	1.5×10^{-12} [a]
k_3	1.3×10^{-2}	1.4×10^{-3}	3.6	1.0
k_5	1.3×10^{-2}	1.4×10^{-3}	0.25	0.080
k_2	0	0	1.6	0.30

[a] In units of mL $site^{-1}$ min^{-1}.

filtered through dry 0.4-μm Bio-Rad Unipore membranes. The filtrates were kept on ice until assayed. Unless noted otherwise in figure legends, each time point is the average from three or more separate experiments. Prior to each experiment, the cell densities were adjusted to the same OD_{600} reading in a double-beam spectrophotometer. The values of $k_1[C]$ in Figure 6 are calculated from the initial slopes of three or more experiments.

Eclipse Kinetics. The following represents a modification of the original procedure (Newbold & Sinsheimer, 1970b). The growth and preparation of the cells and virus preincubation were the same as above. During the last 15 min of the virus incubation period at 37 °C, the washed cells were preincubated at 15 °C. Then, equal volumes of cells and diluted virus were mixed, and adsorption was allowed to proceed for usually 30 min (1.0×10^9 cells/mL and 0.5×10^9 PFU/mL). Aliquots from the C/1 and C/φX reaction tubes were centrifuged for 1 min in an Eppendorf centrifuge, and the supernatant solutions were kept on ice to determine the concentration of unbound virus. After dilution of another aliquot from the C/1 adsorption tube into SVB in ice for the zero-time point, the eclipse reaction was initiated by dilution into SVB at the desired temperature. Aliquots from the eclipse reaction mixture were quenched by a 1:50 dilution in EDTA–borate elution buffer in ice. Two aliquots from the zero-time tube were quenched, one at the beginning and one at the end of the reaction, and their titers were averaged for use in calculating the fraction of PFU's per milliliter at each time point. Temperature for all kinetic experiments was controlled to ±0.01 °C.

Digital Computer Techniques. The use of CSMP III for the simultaneous solution of the differential equations is described by Incardona (1983b). The computations were performed on the IBM 370/3031 at The University of Tennessee Computing Center in Knoxville and on the DEC 1170 in the Academic Computer Center at the University of Tennessee Center for the Health Sciences.

Electron Microscopy. The samples were adsorbed to parlodion-coated electron-microscope grids that were freshly glow-discharged. They were then stained with 4% aqueous uranyl acetate and viewed in a Philips EM 301 electron microscope operated at 80 kV.

Results

Does Reversible Binding Precede Viral Eclipse? In previous studies on the adsorption kinetics of φX174, dilution of the virus–cell mixture was used to quench the binding reaction (Fujimura & Kaesberg, 1962; Newbold & Sinsheimer, 1970b; Segal & Dowell, 1974). If, however, binding is reversible, changing concentrations of reactants and products could shift the equilibrium. We therefore tested the effect of dilution on the level of infectious wild-type virus in supernatant solutions after removal of cells by centrifugation. At every time interval sampled, the fraction of initial PFU's per milliliter was 2–3-fold higher in aliquots that were diluted 100-fold into SVB at 2 °C prior to centrifugation at 12000*g* than in those centrifuged directly. This could be due to dissociation of virus from the cells during dilution or, as suggested below, to release of virus–LPS complexes from the cell. In this study, as well as a previous one (Incardona, 1983b), we filtered undiluted aliquots through a 0.4-μm filter. Filtration, however, does not separate free virus from that bound to outer membrane fragments that pass through the filter. This means that virus titers of the filtered aliquots would be the combined concentrations of free virus and soluble virus–receptor complexes.

The unusual binding curves of purified φX to *E. coli* not only ruled out a simple reversible binding mechanism but proved very restrictive for as complex a model as eq 1. Only two sets of values for the six rate constants could be found which generated curves that fit the experimental data equally well. The similarity of these two cases makes it difficult to distinguish between them at 15 °C. One set (see Table I) suggests that the Fcs70 mutation does not alter the binding of φX to either cell-bound or free receptors but reduces the rate at which virus–receptor complexes are released from the cells at that temperature. The other set of constants predicts the opposite effect of the Fcs70 mutation; the release rate (k_4) is not altered, but binding to free receptors is reversible (k_2 not equal to zero).

Despite these similarities, the two sets of rate constants lead to a small but experimentally measurable difference in the theoretical binding curves. If a higher concentration of free receptors is present at the time that virus is mixed with the cells, the model predicts a significant increase in the plateau level for the $k_2 = 0$ case. One would expect such a situation to exist if binding experiments were performed with crude lysates. From the standpoint of the binding studies, the major contaminating component in lysates would be LPS-containing outer membrane fragments. In Figure 1B, the plateau level of PFU's for Eam3Fcs70 crude lysates is at 9% while that for purified virus is at 6%. The irreversible model ($k_2 = 0$) predicts that doubling the initial concentration of free receptors from 5.5% to 10% generates curves that closely fit the data points (solid lines), but the reversible model ($k_2 = 0.022$ min^{-1}) shows no significant increase in the plateau level of PFU's even with the free receptor concentration at 15% (dashed lines). However, the fit of the computer-generated curves to the Eam3Fcs70 data at the lower cell density (Figure 1A) for the $k_2 = 0$ case is not very gratifying. A more stringent experimentl test will be required to distinguish unequivocally between these two possibilities.

However, the two-step, two interconnecting pathway model accounts for the major features of the observed binding curves for both Eam3 (data not shown) and Eam3Fcs70 at 15 °C. Thus, we feel confident in concluding that some step, or steps, between the initial attachment of φX174 to cell bound receptors and the irreversible eclipse reaction is itself irreversible. Furthermore, the Fcs70 mutation does not lead to an increased

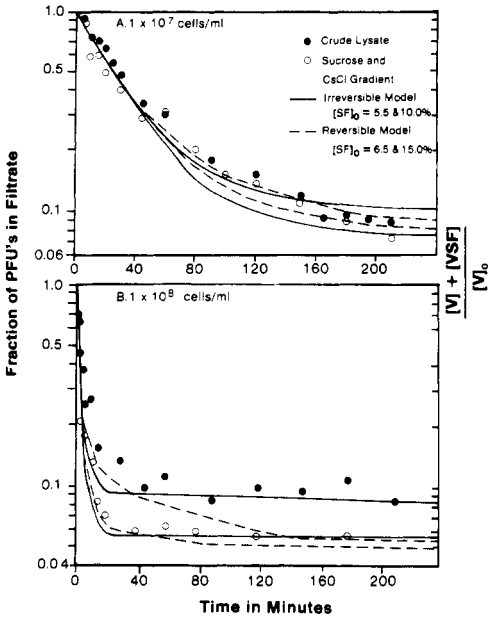

FIGURE 1: Effect of purification on *Eam3cs70* adsorption at 15 °C. The virus was diluted in pH 8.1 (25 °C) SVB to an initial concentration of approximately 1×10^7 PFU/mL: (●) crude lysate; (○) average of data on virus preparation after sucrose gradient step and subsequent CsCl gradient step. In the computer-generated curves of the model of eq 1, the initial cell-bound site concentration $[S]_0$ was 10^4 times the cell concentration. The following rate constants were used: $k_1 = 3.0 \times 10^{-13}$ min^{-1} ml site^{-1}; $k_0 = 1.0 \times 10^{-3}$ min^{-1}. (—) $k_2 = 0$; $k_4 = 1.0 \times 10^{-4}$ min^{-1}; $k_3 = k_5 = 1.4 \times 10^{-3}$ min^{-1}; $[SF]_0 = 5.5\%$ and 10.0% of $[S]_0$ or $k_2 = k_4 = k_3 = k_5 = 0$ and same values for $[SF]_0$. (--) $k_2 = 2.2 \times 10^{-2}$ min^{-1}; $k_4 = 1.0 \times 10^{-3}$ min^{-1}; $k_3 = k_5 = 0.70 \times 10^{-3}$ min^{-1}; $[SF]_0 = 6.5\%$ and 15% $[S]_0$. (A) 1×10^7 cells/mL; (B) 1×10^8 cells/mL.

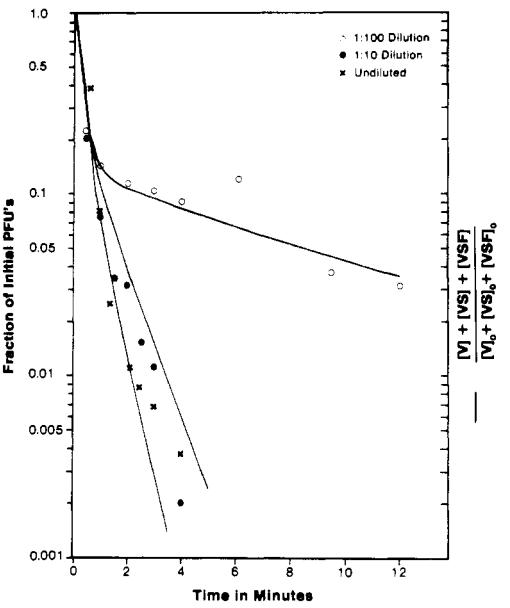

FIGURE 2: Effect of dilution on wild-type eclipse kinetics at 37 °C. Virus was diluted to 1×10^9 PFU/mL in pH 8.1 (25 °C) SVB, preincubated at 37 °C for 15 min, and mixed with an equal volume of cells to give a final concentration of 1×10^9 cells/mL. After 30 min for adsorption at 15 °C, the virus–cell complexes were shifted to 37 °C for the eclipse reaction. (○) 1:100 dilution; (●) 1:10 dilution; (×) undiluted. The following values were used in the computer-generated curves: $k_1 = 1.5 \times 10^{-12}$ min^{-1} ml site^{-1}; $k_0 = k_4 = 5.0 \times 10^{-2}$ min^{-1}; $k_2 = 1.6$ min^{-1}; $k_3 = 3.6$ min^{-1}; $k_5 = 0.25$ min^{-1}; $[V]_0 = 0$; $[S]_0 = 9.7 \times 10^{12}$ sites/mL; $[SF]_0 = 1.30 \times 10^{12}$ sites/mL; $[VS]_0 = 2.95 \times 10^8$ complexes/mL; $[VSF]_0 = 4.50 \times 10^7$ complexes/mL; $[ES]_0 = 1.44 \times 10^8$ complexes/mL; $[ESF]_0 = 1.66 \times 10^7$ complexes/mL. The initial concentrations were reduced by the corresponding factor for the diluted curves.

rate of dissociation from cell-bound receptors.

Molecular Basis of the Nonlinear Eclipse Kinetics. The technique for measuring the rate of the eclipse reaction of ϕX bound to intact cells does not yield a simple first-order plot (Newbold & Sinsheimer, 1970b; Incardona, 1974), as would be expected for a single two-step reaction pathway. The original procedure of Newbold & Sinsheimer (1970b) involved a 100-fold dilution of virus–cell complexes made at 15 °C to initiate the eclipse reaction at a higher temperature. Since we encountered an unexpected effect of dilution on ϕX binding, we also examined the effect of dilution on the eclipse kinetics. At the end of a 30-min adsorption period at 15 °C with a crude lysate of wild-type ϕX and *E. coli* C/1 cells, the reaction mixture was either transferred undiluted into a dry tube that had been prewarmed in a 37 °C water bath or diluted by a factor a 1:10 or 1:100 in SVB at 37 °C. In each case, aliquots were quenched by the usual 1:50 dilution into EDTA elution buffer in ice. The results are shown in Figure 2. One can see that a dramatic reduction of the nonlinearity is accomplished if the complexes are shifted to the higher temperature without diluting them or with a 1:10 dilution.

An explanation for the reduced eclipse rate at the higher dilution can be found in our reaction model in eq 1. The solid lines in Figure 2 are computer-generated curves from experimentally determined values of k_1, k_3, and k_5. With regard to the latter, we assumed that the slow component of the 1:100 dilution data was due to the eclipse reaction of virus bound to free receptors. Therefore, an estimate of k_5 could be obtained from a straight line drawn through the data points between 2 and 12 min and extrapolation of the line to the origin. The initial concentrations of all reactants, intermediates, and products were taken from computer-generated curves simulating the adsorption conditions at 15 °C prior to initiating the eclipse reaction. This left only k_0, k_4, and k_2 to adjust by trial and error. We assumed k_0 and k_4 were identical, as was the case at 15 °C for *Eam3* (see Table I). However, we assigned a larger value to these constants due to the higher temperature of the eclipse experiment. After the general shape of the curves was established by adjusting these three rate constants, minor alterations were made in k_3, k_5, and the initial concentrations of VS and VSF to get the fit shown in Figure 2.

The most striking conclusion from this curve fitting is that a nonzero value for k_2, the dissociation rate for free virus–receptor complexes, is required to account for the large difference beween the data obtained at the three initial concentrations of the system. If k_2 is set to zero in the model, a *single* curve similar to that fitted to the 1:100 dilution data in Figure 2 is generated at all initial concentrations. This is a result of both eclipse reactions (on cell-bound and free receptors) being first-order and independent of reactant concentrations. However, if ϕX dissociates from free virus–receptors complexes (k_2 not equal to zero), the released virus can rebind to cells and eclipse on cell-bound receptors. Since the rate of virus binding to cell-bound receptors is a function of cell concentration, the binding reaction is rate limiting at a 1:100 dilution due to the low concentration of cells in the reaction mixture. This binding rate is approximately the same as the eclipse rate (k_5) on released receptors. Thus, free virus that rebinds to cells and virus bound to free or released receptors undergo that eclipse reaction at approximately the same slow rate after the first few minutes of the experiment.

We have made one assumption in fitting our model to the wild-type eclipse data: the slow component in the 1:100 dilution of the system is due to the eclipse reaction of ϕX bound

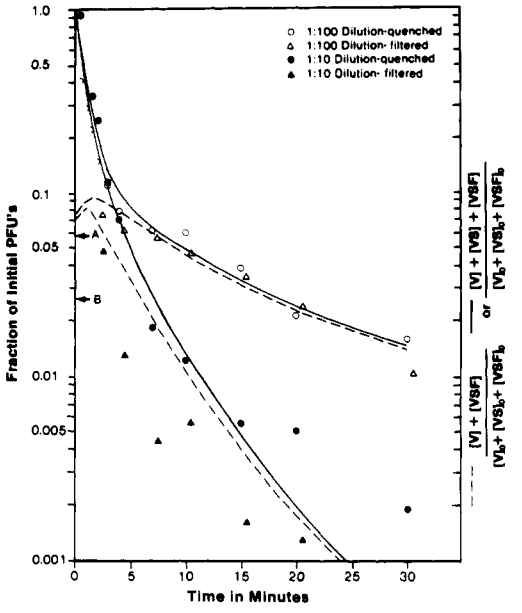

FIGURE 3: Effect of dilution on E*am*3F*cs*70 eclipse kinetics at 37 °C. Virus was diluted to 1 × 10^8 PFU/mL in pH 8.1 (25 °C) SVB, preincubated at 37 °C for 30 min, and mixed with an equal volume of cells to give a final cell concentration of 1 × 10^9 cells/mL. After 15 min for adsorption at 15 °C, an aliquot of the virus–cell complexes was shifted to 37 °C by a 1:100 dilution, and after 45 min another aliquot was shifted to 37 °C by a 1:10 dilution: (○) 1:100 dilution quenched; (△) 1:100 dilution filtered; (●) 1:10 dilution quenched; (▲) 1:10 dilution filtered; A and B are the PFU's per milliliter in supernatant solutions after 15- and 45-min adsorption at 15 °C, respectively. The following values were used in the computer-generated curves: k_1 = 1.5 × 10^{-12} min^{-1} mL $site^{-1}$; $k_0 = k_4$ = 5.0 × 10^{-2} min^{-1}; k_2 = 0.30 min^{-1}; k_3 = 1.0 min^{-1}; k_5 = 0.08 min^{-1}, $[V]_0$ = 0; $[S]_0$ = 9.7 × 10^{11} sites/mL; $[SF]_0$ = 8.5 × 10^{10} sites/mL; $[VS]_0$ = 4.5 × 10^6 complexes/mL; $[VSF]_0$ = 3.4 × 10^5 complexes/mL; $[ES]_0$ = 9.6 × 10^4 complexes/mL; $[ESF]_0$ = 5.4 × 10^3 complexes/mL. The initial concentrations were reduced 10-fold for the 1:100 dilution curves.

to free receptors. Additional experiments were performed to test this assumption. First, the same experiment was repeated with a purified preparation of E*am*3F*cs*70. The model predicts a difference should also occur between a 1:10 and 1:100 dilution if the *cs*70 mutation alters only the rates of the two eclipse reactions (k_3 and k_5). We, therefore, estimated k_3 and k_5 from the slopes of straight lines drawn through the early and late time points of the 1:100 dilution data, respectively (open circles in Figure 3). Since the other rate constants were identical with those used for wild-type φX, trial and error adjustment of only k_2 was needed to fit the curve to the data at both dilutions (solid lines and open and closed circles in Figure 3). As before, initial concentrations were established by computer-generated data with the same values for the E*am*3F*cs*70 rate constants at 15 °C as those used in Figure 1.

A second test of the assumption involves measuring the PFU's per milliliter in filtered aliquots taken during the course of an eclipse experiment. If the slow component in the eclipse kinetics is due to virus bound to small outer membrane fragments, the same PFU's per milliliter found in the quenched samples should be present in filtered samples. Therefore, undiluted aliquots were also filtered during the course of the experiment (open and closed triangles in Figure 3). A good fit to the 1:100 dilution data was obtained for the total concentration of free virus and uneclipse virus bound to released receptors (dashed lines in Figure 3). The lack of fit to the 1:10 dilution data from the filtrates may be due to the release of larger virus–receptor fragments by the lower dilution and some of them being retained on the filters. In the 1:100 dilution

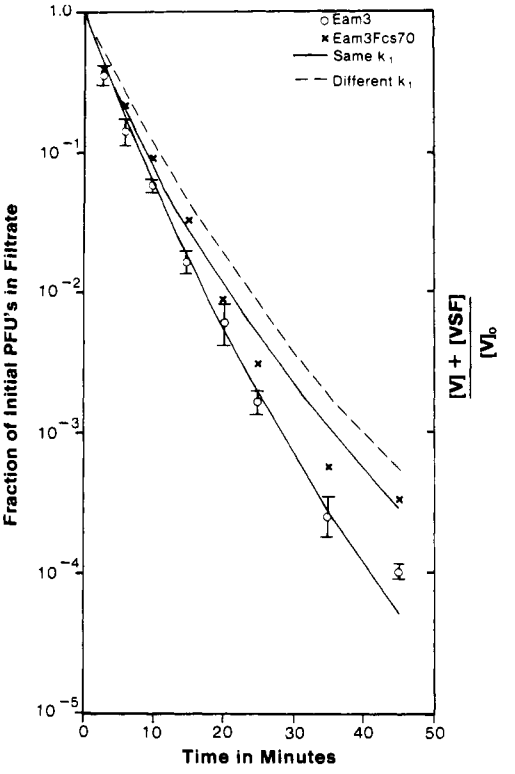

FIGURE 4: Adsorption kinetics of purified virus at 37 °C in pH 8.1 (25 °C) SVB. The initial virus concentration was approximately 1 × 10^7 PFU/mL, and initial cell density was 2 × 10^7 cells/mL. (○) Average of sucrose gradient purified E*am*3, J-F *del* 3, and J-F *ins* 11; (×) average of sucrose gradient and CsCl gradient purified E*am*3F*cs*70. The following values were used for both the E*am*3 and E*am*3F*cs*70 curves: (—) k_1 = 1.5 × 10^{-12} min^{-1} mL $site^{-1}$; $k_0 = k_4$ = 1.5 × 10^{-2} min^{-1}; $[S]_0$ = 2.0 × 10^{11} sites/mL; $[SF]_0$ = 5% of $[S]_0$. For the E*am*3 curve, k_2 = 1.6 min^{-1}, k_3 = 3.6 min^{-1}, and k_5 = 0.25 min^{-1}. For the E*am*3F*cs*70 curve, k_2 = 0.30 min^{-1}, k_3 = 1.0 min^{-1}, and k_5 = 0.08 min^{-1}. The following values were used in the E*am*3F*cs*70 curve: (– –) k_1 = 1.2 × 10^{-12} min^{-1} mL $site^{-1}$; k_2 = 1.6 min^{-1}. All other values were the same as those used in the solid E*am*3F*cs*70 curve.

experiment, the close match of the PFU's per milliliter in the filtered and quenched samples rules out the possibility that the slow component is due to reactions involving cell-bound virus since all cell-bound virus would be retained on the filter.

This is further demonstrated in a second experiment with the same preparation of E*am*3F*cs*70. The adsorption mixture was centrifuged at room temperature for 1 min in an Eppendorf centrifuge. The supernatant solution was removed, the pellet was resuspended in the same volume of SVB kept at 15 °C, and both samples were maintained at 15 °C until initiating the eclipse reaction at 37 °C. The results with a 1:10 dilution of the resuspended pellet were identical with those in Figure 3, while a 1:10 dilution of the supernatant solution yielded mainly the slow component of the curve in Figure 3 (data not shown). Thus, the slow component is due to the eclipse of virus attached to receptor structures not bound to cells.

Binding Kinetics at 37 °C. Another unusual feature that we observed in φX binding data is the nonlinearity of the pseudo-first-order plots at 37 °C. At a cell density of 2.0 × 10^7, one must follow the reaction through 4 log units of decreasing PFU's per milliliter to convincingly demonstrate the nonlinearity. This is illustrated in Figure 4 with purified preparations of both E*am*3 and E*am*3F*cs*70. The nonlinearity provides us with another test for our model since the eclipse experiments in Figures 2 and 3 establish values for all rate constants at 37 °C. The solid lines in Figure 4 are the com-

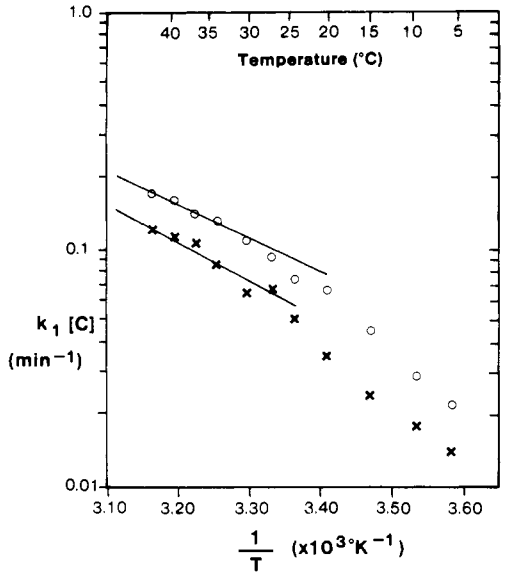

FIGURE 5: Effect of temperature on adsorption in SVB. The initial virus concentration was approximately 1×10^7 PFU/mL, and cell concentration was 1×10^7 cells/mL. (O) E*am*3; (×) E*am*3F*cs*70.

puter-generated curves of these same values except for those assigned to k_0 and k_4, the constants associated with the release of receptor sites from the cell. These values had to be decreased from 0.050 to 0.015 min^{-1} to accomodate a small, but probably significant, difference in design between the two types of experiments. In binding experiments the cells are incubated in SVB at 37 °C for 15 min prior to the start of the reaction at that temperature. However, the cells are at *15 °C* for 30 min prior to the shift to 37 °C in the eclipse experiments. In a study by Rothfield & Pearlman-Kothencz (1969), the release rate of LPS-containing outer membrane fragments decreased after 15 min at 37 °C. Since our model at this stage of development cannot mathematically account for such a change in rate during the course of our experiments, a realistic approximation is the assignment of different values to the rate constants themselves for the two types of experiments. Thus, the release rate constant is given a larger value in simulating the eclipse kinetic data than in simulating the binding data at 37 °C.

Effect of Temperature on Binding. Having established that binding to cell-bound receptors is irreversible, we examined the effect of temperature on k_1, the binding rate constant. Crude lysates of wild-type ϕX, E*am*3, and F*cs*70 were used, and the rate constants were calculated from initial slopes. The Arrhenius plot in Figure 5 shows that the lower binding rate exhibited by the F*cs*70 mutant at 37 °C (Figure 4) persists at all temperatures down to 6 °C. We therefore considered the possibility that the F*cs*70 mutation decreases k_1 instead of k_2 from the wild-type values. The dashed line in Figure 4 is the computer-generated curve with the lower k_1 obtained from the initial slope of the F*cs*70 data and the wild-type value for k_2. The failure of the curve to fit the data appears to rule out any significant alteration of k_1 by the F*cs*70 mutation so the observed differences in the initial slopes are most likely due to the lower value for k_2.

As for the nonlinearity of the Arrhenius plot, we can only say that it is not due to the large change in pH that is characteristic of Tris buffers over the temperature range of the measurements. Binding curves at 37 °C were obtained in SVB adjusted to different pHs that covered the range from 7.0 to 8.8 at that temperature. The initial slopes were constant between pH 7.0 and pH 8.5 and decreased slightly at higher pHs. The most likely explanation lies in the effect of temperature on the other rate constants, but no attempt was made to explore this with computer-generated curves based on our model. An activation enthalpy of 22.5 J/mol for binding can be estimated from the linear portion of the Arrhenius plot above 20 °C.

Table II: Effect of Cations on Binding

divalent	monovalent	k_1 ($\times 10^{-9}$ min^{-1} mL cell^{-1})
	SVB[a]	4.8
1.0 mM Ca^{2+}	0	3.5
0	100 mM K^+	2.0
0.5 mM Ca^{2+}	100 mM K^+	2.0
1.0 mM Ca^{2+}	100 mM K^+	5.0
5.0 mM Ca^{2+}	100 mM K^+	6.6
10.0 mM Ca^{2+}	100 mM K^+	6.6
5.0 mM Mg^{2+}	100 mM K^+	6.9

[a] Consists of 10 mM Tris, pH 7.8, 1.0 mM $CaCl_2$, 0.5 mM $MgSO_4$, 20 mM NaCl, and 100 mM KCl.

Cation Requirement for Binding. Although Fujimura & Kaesberg (1962) demonstrated a divalent cation requirement for binding of ϕX to *E. coli*, their studies were done at 37 °C where both binding and eclipse reactions are functional. We therefore examined the effect of various mono- and divalent cations on the binding reaction alone by measuring the initial slopes of binding curves with purified E*am*3F*cs*70 at 15 °C. In a preliminary experiment, a series of Tris buffers at the same concentration as SVB (10 mM) were prepared so that their pHs would be 7.8 at that temperature. Each contained one of the mono- or divalent cation salts that are present in the complete SVB. Either divalent cation alone gave a significantly faster rate than the monovalent cations even though their concentrations were 20–200-fold lower. Yet, none of the rates were as fast as SVB (see first three entries in Table II). One likely reason for the synergistic effect of these cations is that the monovalent salts provide sufficient ionic strength to reduce the electrostatic repulsion between the cells and ϕX, while the divalent cations play a more specific role in binding to the LPS receptors. We found that the combination of 1.0 mM Ca^{2+} and 100 mM K^+ supports the same rate as does SVB (Table II) and that this rate is close to the maximum observed at a concentration of 5.0 mM Ca^{2+}. It can also be seen from Table II that Mg^{2+} seems equally as effective as Ca^{2+}.

Evaluation of Reaction Pathway Model. The unusual features of the ϕX174 adsorption and eclipse data provide fairly stringent tests of a reaction pathway model. First, the 15 °C binding curves at two cell densities clearly rule out that a reversible binding step immediately preceeds the eclipse reaction on cell-bound receptors. Prior to testing our model in eq 1, we tried several other models that featured reversible binding steps. In every instance they predicted that the fraction of initial PFU's per milliliter in the filtrates should not reach the same level at the two cell densities used in the experiments. It is clear from Figure 1 that the experimental values do reach the same level. The key feature of our model that accounts for this aspect of the binding data is the release of both unoccupied and occupied receptor sites from the cell. The latter was verified by examination of filtrates in the electron microscope. One can see fragments of membranes attached to the ϕX particles in the filtrates taken after a 1-h incubation period at 15 °C with *E. coli* C/1 cells (Figure 6A) but not with the resistant strain, C/ϕ*X* (Figure 6B). Second, the large difference in slope when the eclipse reaction is initiated by dilution to different cell densities (Figures 2 and 3) requires reversible binding to free receptor sites. Independent evidence

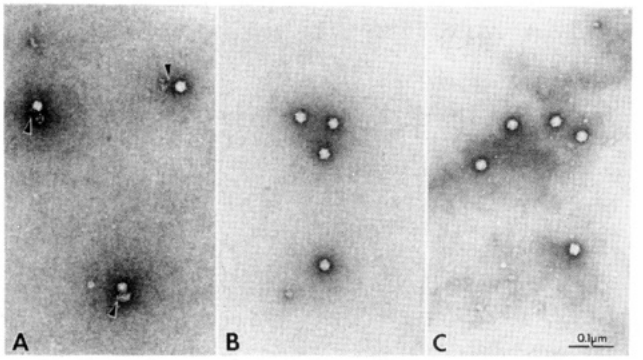

FIGURE 6: Electron micrographs of released virus–receptor complexes. (A) Filtrate from *E. coli* C/1 (sensitive) cells incubated with ϕX E*am*3F*cs*70 for 1 h at 15 °C. Note membrane fragments (arrowheads) associated with each phage particle. (B) Filtrate from *E. coli* C/ϕX (resistant) cells treated as in (A). (C) An aliquote of filtrate in (A) was incubated at 37 °C for 30 min. Note the dissociation of membrane fragments from the phage.

for the reversible binding of ϕX to released receptors was also obtained by electron microscopy. We simply took an aliquot of the filtrate that contained the virus–receptor complexes seen in Figure 6A and incubated it for 30 min at 37 °C prior to applying a sample to the grids. As can be seen in Figure 6C, the membrane fragments are no longer attached to ϕX. Third, the binding curves at 37 °C are fairly sensitive to the values of k_0 and k_4, particularly in the context of the lower F*cs*70 eclipse rates. An approximately 3-fold decrease in release rates from the values used to fit the eclipse data at 37 °C was all that was required to obtain the fit to the binding data shown in Figure 4. Independent verification of this decrease in rate with time at 37 °C can be found in the estimated change in slope for excretion of labeled LPS observed by Rothfield & Pearlman-Kothencz (1969; Figure 2).

Discussion

The success of the model in accounting for these diverse features in the experimental data suggests that the main concepts of the model are valid. Moreover, its essential features are supported by electron microscopy. This leads us to speculate that ϕX binding to cells is irreversible because more than one viral vertex is interacting with LPS receptors. Since the dissociation constant for a multivalent ligand is the product of the dissociation constants for the individual binding interactions, only two or three vertices would be required for irreversible attachment of the phage to the cell. Electron micrographs of freeze-etch replicas prepared from infected *E. coli* C cells show ϕX virions buried into the cell surface to almost half their diameters (Brown et al., 1971), suggesting that up to six vertices are interacting with their receptors. Thus, ϕX may have the simplest binding mechanism—multiple copies of a single attachment structure. The use of multiple attachment structures appears to be a general feature with viruses although some may use more than one kind of attachment structure.

With regard to the physiological defects induced by the F*cs*70 mutation, the curve fitting of our model to the binding and eclipse data provides good estimates of the relevant rate constants. It is clear from the summary of values given in Table I that the mutant is defective in the eclipse reaction on cell-bound receptors (k_3), even at permissive conditions. Moreover, this defect persists in soluble virus–receptor complexes (k_5) and should be detectable by in vitro assays (Incardona & Selvidge, 1973). On the other hand, no significant difference in the initial binding to cell-bound receptor sites (k_1) occurs. As shown in Figure 5, the lower binding rate exhibited by E*am*3F*cs*70 could not be accounted for by a lower value for k_1 but could be explained by a lower dissociation rate from soluble receptor sites (k_2). This is consistent with the fact that attachment of ϕX to cells is a diffusion-limited reaction, as shown by the close agreement between the experimentally determined k_1 and that calculated from the diffusion coefficient (Incardona, 1983a). Also, the $\Delta H^{\ddagger}$ calculated from the slope of the Arrhenius plot for k_1, 22.5 J/mol (Figure 6), is in good agreement, with the $\Delta H^{\ddagger}$ of 20.9 J/mol for the viscosity of water. This indicates that the temperature effect on the rate constant is the same as that for the diffusion coefficient (Incardona, 1983a). Finally, the mutation does not change the binding to cell-bound receptor sites from an irreversible reaction to a reversible one. The combined decrease in k_3 and k_2 in F*cs*70 provides a molecular explanation for this mutant's failure to begin the eclipse phase at the nonpermissive temperature. Since its eclipse rate is lower than that of wild-type virus, the probability of it being released from the cell as a virus–receptor complex is greater for wild-type virus. However, the released F*cs*70–receptor complex does not dissociate as rapidly as that formed with wild-type virus. Thus, the probability of F*cs*70 being inactivated by the eclipse reaction on released receptors is greater than wild-type virus, so released F*cs*70 cannot reinfect new cells as efficiently as wild-type does. Our primary interest lies in characterizing those viral functions associated with the capsid proteins of ϕX174. We have focused our efforts on the process by which the phage delivers its genome through the bacterial outer membrane, since molecular genetic techniques are available for establishing structure–function relationships in this system. Thus, a knowledge of the reactions that take place once the virus encounters the cell surface is important for our analysis. The binding and eclipse data clearly demonstrate that a complication exists in the early steps of the ϕX infection pathway. However, our model provides a simple explanation for the unusual features in the data. It also supports the concept that relatively few rate constants are required to characterize the interaction of ϕX with its LPS receptor site. Furthermore, the analysis of the F*cs*70 data shows that the values for these constants can be extracted from the data with sufficient accuracy to establish the functional alterations of a mutant allele.

Acknowledgments

We acknowledge the use of The University of Tennessee Computer Center in Knoxville, as well as the Academic Computer Center at the University of Tennessee Center for the Health Sciences. Technical assistance at various stages was provided by Marsha Brown, Robbie Kimbough, and Susan Jennings. Their persistent attention to detail was an important factor in this work. In the case of the electron microscopy, we would like to acknowledge Loretta Hatmaker and Kathy Troughton. Certain portions of the data were submitted by Blake Barton and Brian Anthony to the Biology Department, Christian Brothers College, in partial fulfillment of the requirements for the B.S. degree.

References

Aoyama, A., Hamatake, R. K., & Hayashi, M. (1981) *Proc. Natl. Acad. Sci. U.S.A. 78*, 7285–7289.

Benbow, R. M., Hutchison, C. A., III, Fabricant, J. D., & Sinsheimer, R. L. (1971) *J. Virol. 7*, 549–558.

Brown, D. T., MacKenzie, J. M., & Bayer, M. E. (1971) *J. Virol. 7*, 836–846.

Burgess, A. B. (1969) *Proc. Natl. Acad. Sci. U.S.A. 64*, 613–617.

Edgell, M. H., Hutchinson, C. A., III, & Sinsheimer, R. L. (1969) *J. Mol. Biol. 42*, 547-557.
Fujimura, R., & Kaesberg, P. (1962) *Biophys. J. 6*, 433-449.
Hutchison, C. A., III, Middleton, J. H., & Edgell, M. H. (1972) *Biophys. J. 12*, 31a.
Incardona, N. L. (1974) *J. Virol. 14*, 469-478.
Incardona, N. L. (1981a) *J. Virol. 39*, 510-518.
Incardona, N. L. (1981b) *Recept. Recognit. Ser. B. 8*, 157-167.
Incardona, N. L. (1983a) *J. Theor. Biol. 104*, 693-699.
Incardona, N. L. (1983b) *J. Theor. Biol. 105*, 631-645.
Incardona, N. L., & Selvidge, L. (1973) *J. Virol. 11*, 775-782.
Incardona, N. L., & Müller, U. R. (1985) *J. Mol. Biol. 181*, 479-486.
Jazwinski, S. M., Lindberg, A. A., & Kornberg, A. (1975a) *Virology 66*, 268-282.
Jazwinski, S. M., Marco, R., & Kornberg, A. (1975b) *Virology 66*, 294-305.
Muhlradt, P. F., & Menzel, J. (1974) *Eur. J. Biochem. 43*, 533-539.
Müller, U. R., & Wells, R. D. (1980) *J. Mol. Biol. 141*, 1-24.
Newbold, J. E., & Sinsheimer, R. L. (1970a) *J. Mol. Biol. 49*, 49-66.
Newbold, J. E., & Sinsheimer, R. L. (1970b) *J. Virol. 5*, 427-431.
Osborn, M. J., Rick, P. D., & Rasmussen, N. S. (1980) *J. Biol. Chem. 255*, 4246-4251.
Rothfield, L., & Pearlman-Kothencz, M. (1969) *J. Mol. Biol. 44*, 477-492.
Rueckert, R. R., & Zillig, W. (1962) *J. Mol. Biol. 5*, 1-9.
Sanger, F., Coulson, A. R., Friedmann, T., Air, G. M., Barrell, B. G., Brown, N. L., Fiddes, J. C., Hutchison, C. A., III, Slocombe, P. M., & Smith, M. (1978) *J. Mol. Biol. 125*, 225-246.
Segal, D. J., & Dowell, S. E. (1974) *J. Virol. 14*, 1115-1125.
Siden, E. J., & Hayashi, M. (1974) *J. Mol. Biol. 89*, 1-16.

all-trans-Retinoids and Dihydroretinoids as Probes of the Role of Chromophore Structure in Rhodopsin Activation†

Roger D. Calhoon and Robert R. Rando*
Department of Pharmacology, Harvard Medical School, Boston, Massachusetts 02115
Received March 20, 1985

ABSTRACT: The absorption of a photon of light by rhodopsin results in the cis to trans isomerization of the 11-*cis*-retinal Schiff base chromophore. In the studies reported here, an attempt is made to determine the mechanism of the energization of rhodopsin as it relates to the chemistry of the isomerization process and the geometrical state of the chromophore. Studies were performed with vitamin A analogues to probe this mechanism. Both 11-*cis*-7,8-dihydroretinal and 9-*cis*-7,8-dihydroretinal form bleachable pigments when combined with opsin. Photolysis of these pigments in the presence of G-protein results in the activation of the latter as revealed by its GTPase activity. Phosphodiesterase is also activated when it is included in the incubation. Therefore, the possibility that rhodopsin is energized by mechanisms involving photochemically induced charge transfer from the protonated Schiff base to the β-ionone ring can be discarded. Further studies were conducted with *all-trans*-vitamin A derivatives to determine if these compounds can form the GTPase-activating state R*, a situation that is possible, in principle, by microscopic reversibility. Neither *all-trans*-retinal nor its oxime, when incubated with bovine opsin in the dark, caused activation of the GTPase, requiring at least a 5 kcal/mol energy gap between them. Furthermore, stoichiometric adducts of *all-trans*-retinoids and opsin were also unable to mediate activation of the GTPase. Since both *all-trans*-15,16-dihydroretinylopsin and *all-trans*-retinoylopsin possess an *all-trans*-retinoid permanently adducted to opsin, it can be concluded that the *all-trans*-retinoid chromophore–opsin linkage may be necessary but not sufficient to achieve activation of the visual pigment.

The absorption of a photon of light by rhodopsin results in the isomerization of the 11-*cis*-retinal protonated Schiff base chromophore to its all-trans congener (Hubbard & Kropf, 1958). Concomitant with this isomerization, conformational changes in the protein take place resulting eventually in the hydrolysis of the protonated Schiff base of *all-trans*-retinal generating the aldehyde and opsin (Wald, 1968). On the way to opsin formation, one of the rhodopsin conformers, R*,[1] probably identical with or arising from the spectroscopically defined state metarhodopsin II (Parkes et al., 1979; Calhoon et al., 1981), causes the exchange of GTP for GDP in the G-protein (Fung & Stryer, 1980), which in turn activates a cyclic GMP phosphodiesterase (Fung et al., 1981). The G-protein eventually hydrolyzes the GTP to GDP, returning the G-protein to an inactive state with respect to phosphodiesterase activation. Since enzymatic activity of GTP hydrolysis is the activity measured in the work reported here, we refer to the enzyme as "GTPase" rather than emphasizing the protein's role as mediator of activation of the phosphodiesterase, as implied by the term "G-protein". The hydrolysis of cGMP is the only metabolically significant event known to

† This work was supported by U.S. Public Health Service Research Grant EY-03624 from the National Institutes of Health. R.D.C. was supported by U.S. Public Health Service Training Grant NS-07009.
* Correspondence should be addressed to this author.

[1] Abbreviations: CHAPSO, 3-[(3-cholamidopropyl)dimethylammonio]-2-hydroxy-1-propanesulfonate; Meta, metarhodopsin; PIPES, piperazine-*N*,*N*'-bis(2-ethanesulfonic acid); Rh, rhodopsin; ROS, rod outer segments; R*, GTPase-activating state of rhodopsin; Tris, tris(hydroxymethyl)aminomethane.

0006-2960/85/0424-6446$01.50/0